

# Cell Type-Specific Neuroprotective Activity of Untranslocated Prion Protein

Elena Restelli<sup>1,2</sup>, Luana Fioriti<sup>1,2</sup><sup>✉</sup>, Susanna Mantovani<sup>1,2</sup>, Simona Airaghi<sup>1,2</sup>, Gianluigi Forloni<sup>2</sup>, Roberto Chiesa<sup>1,2</sup><sup>\*</sup>

**1** Dulbecco Telethon Institute, Milan, Italy, **2** Department of Neuroscience, Mario Negri Institute for Pharmacological Research, Milan, Italy

## Abstract

**Background:** A key pathogenic role in prion diseases was proposed for a cytosolic form of the prion protein (PrP). However, it is not clear how cytosolic PrP localization influences neuronal viability, with either cytotoxic or anti-apoptotic effects reported in different studies. The cellular mechanism by which PrP is delivered to the cytosol of neurons is also debated, and either retrograde transport from the endoplasmic reticulum or inefficient translocation during biosynthesis has been proposed. We investigated cytosolic PrP biogenesis and effect on cell viability in primary neuronal cultures from different mouse brain regions.

**Principal Findings:** Mild proteasome inhibition induced accumulation of an untranslocated form of cytosolic PrP in cortical and hippocampal cells, but not in cerebellar granules. A cyclopeptolide that interferes with the correct insertion of the PrP signal sequence into the translocon increased the amount of untranslocated PrP in cortical and hippocampal cells, and induced its synthesis in cerebellar neurons. Untranslocated PrP boosted the resistance of cortical and hippocampal neurons to apoptotic insults but had no effect on cerebellar cells.

**Significance:** These results indicate cell type-dependent differences in the efficiency of PrP translocation, and argue that cytosolic PrP targeting might serve a physiological neuroprotective function.

**Citation:** Restelli E, Fioriti L, Mantovani S, Airaghi S, Forloni G, et al. (2010) Cell Type-Specific Neuroprotective Activity of Untranslocated Prion Protein. PLoS ONE 5(10): e13725. doi:10.1371/journal.pone.0013725

**Editor:** Mark R. Cookson, National Institutes of Health, United States of America


**Received:** July 7, 2010; **Accepted:** October 7, 2010; **Published:** October 28, 2010

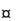
**Copyright:** © 2010 Restelli et al. This is an open-access article distributed under the terms of the Creative Commons Attribution License, which permits unrestricted use, distribution, and reproduction in any medium, provided the original author and source are credited.

**Funding:** This work was supported by Telethon-Italy to RC (TRC08005). L.F. was supported by a fellowship from the Fondazione Monzino. R.C. is an Associate Telethon Scientist (Dulbecco Telethon Institute, Fondazione Telethon). The funders had no role in study design, data collection and analysis, decision to publish, or preparation of the manuscript.

**Competing Interests:** The authors have declared that no competing interests exist.

\* E-mail: roberto.chiesa@marionegri.it

 These authors contributed equally to this work.

 Current address: Department of Neuroscience, Columbia University, New York, New York, United States of America

## Introduction

The cellular prion protein (PrP<sup>C</sup>) is a glycosylphosphatidylinositol (GPI)-anchored cell-surface glycoprotein with unclear function that is expressed at the highest level by neurons in the central nervous system [1,2,3]. Conversion of PrP<sup>C</sup> into an abnormal, misfolded isoform plays a key role in prion diseases, which are invariably fatal neurodegenerative disorders that can arise sporadically, be inherited due to mutations in the gene encoding PrP, or acquired through infection [4].

Research on prion diseases has focused on how perturbations of PrP<sup>C</sup> biosynthesis and metabolism may trigger the neurodegenerative process [5]. PrP<sup>C</sup> is co-translationally translocated into the rough endoplasmic reticulum (ER), where the N-terminal signal peptide (SP) is cleaved, and the GPI anchor is added concurrently with removal of a C-terminal signal sequence. In the ER, the PrP polypeptide undergoes oxidative folding with formation of a single disulphide bond, and the protein is variably modified at two N-glycosylation sites, resulting in a mixture of di-, mono- and unglycosylated forms [6]. After transit in the mid-Golgi, where the immature, core-glycosylated molecules are complex-glycosylated,

PrP is transported through the later compartments of the secretory pathway and delivered to the cell surface, where it resides in lipid rafts [7].

The observation that pharmacological inhibition of the proteasome led to accumulation of an unglycosylated PrP species in neuroblastoma N2a cells [8,9] was interpreted as evidence that part of the newly synthesized PrP was constitutively recognized as misfolded by the ER quality control and diverted to the ER-associated degradation (ERAD) pathway, which implies retrograde transport from the ER lumen to the cytosol, deglycosylation by cytosolic N-glycanases, and proteasomal degradation [10]. Conditions favoring PrP misfolding such as germline or somatic mutations, and/or reduced proteasome function, might therefore lead to accumulation of potentially neurotoxic cytosolic PrP. Consistent with the idea that ERAD-diverted PrP could be neurotoxic if not properly degraded, forced expression of PrP in the cytosol caused degeneration of cerebellar granule neurons, and anatomical and functional abnormalities in the forebrain of transgenic (Tg) mice [11,12,13].

Cytosolic PrP could also be generated by an ERAD-independent mechanism. During PrP biosynthesis a subset of molecules

failed to translocate into the ER lumen and ended up in the cytosol [14,15], because of an intrinsic inefficiency of the PrP signal sequence [16]. The amount of untranslocated PrP increased during ER stress [17,18], providing an alternative mechanism for generating potentially neurotoxic cytosolic PrP [19].

However, several observations undermine the idea that cytosolic PrP is invariably neurotoxic. In non-pathogenic conditions, PrP was found in the cytoplasm of some neuronal populations in the hippocampus, neocortex and thalamus, with no signs of neurodegeneration [20,21,22]. Then too, analysis of cytosolic PrP activity in different cells produced conflicting results: whereas some studies confirmed the toxicity [11,16,23,24,25], others did not [15,26,27], and some brought to light a protective effect against Bax-mediated cell death [28,29]. These observations raised the possibility that cells of different neural origin could differ in their propensity to synthesize PrP in the cytosol, and that this isoform could have cell type-specific biological activities.

To explore this, we investigated cytosolic PrP biogenesis and effects on cell survival in primary neuronal cultures from different mouse brain regions. Here we show that when the proteasome is inhibited, an unglycosylated form of PrP accumulates in cortical and hippocampal cells, but not in cerebellar granule neurons (CGN). This form contains uncleaved signal peptides, indicating that it corresponds to PrP molecules that have escaped translocation into the ER. Consistent with this, an inhibitor of protein translocation increased the amount of cytosolic PrP in cortical and hippocampal neurons, and induced its synthesis in CGNs. Untranslocated PrP was associated with an increase in the resistance of cortical and hippocampal cells to apoptosis, but had no such effect on cerebellar granules. These findings support the conclusion that cytosolic PrP is not neurotoxic, and suggest that selective targeting of nascent PrP to the cytosol might fulfill a neuroprotective function.

## Results

### Untranslocated PrP is Detected in Cultured Cortical and Hippocampal Neurons, but not in Cerebellar Granules

We investigated whether cytosolic PrP was detectable in primary neurons cultured from the neocortex, hippocampus and cerebellum of newborn mice. Because cytosolic PrP is rapidly degraded by the proteasomes [14,15], cells were treated with a panel of different proteasome inhibitors. Lactacystin- $\beta$ -lactone, MG132 (Z-Leu-Leu-Leu-al), ALLN (Ac-Leu-Leu-NorLeu-al) or epoxomicin caused accumulation of an insoluble form of PrP of approximately 27 kDa in cortical and hippocampal neurons (Fig. 1A, middle and bottom panels, and Fig. 1B top panel). This form had a larger molecular mass than mature, unglycosylated PrP in the soluble fractions, and was recognized by an antibody ( $\alpha$ -SP), which selectively reacts with the N-terminal signal peptide of PrP [30] (Fig. 1B, lower panel), indicating that it corresponded to the untranslocated form of cytosolic PrP previously described in transfected cells (hereafter referred to as SP-PrP) [14,15,16,17]. In cortical and hippocampal cells SP-PrP was first detected after 2 h treatment, and reached a maximum within 8 h (data not shown) which, based on quantitative evaluation of Western blots, corresponded to approximately 10% of total PrP. Consistent with previous findings [14,15], SP-PrP was not detected in proteasome inhibitor-treated CGN (Fig. 1A, top panel). PrP levels were similar in the different neuronal cultures, ruling out that the failure to detect SP-PrP in CGN was due to lower PrP expression.

During acute ER stress, PrP is prevented from translocating into the ER and is routed to the cytosol [17,18]. To see whether proteasome inhibitors activated ER stress pathways in neurons, we followed the splicing of X-box binding protein 1 (XBP1) mRNA

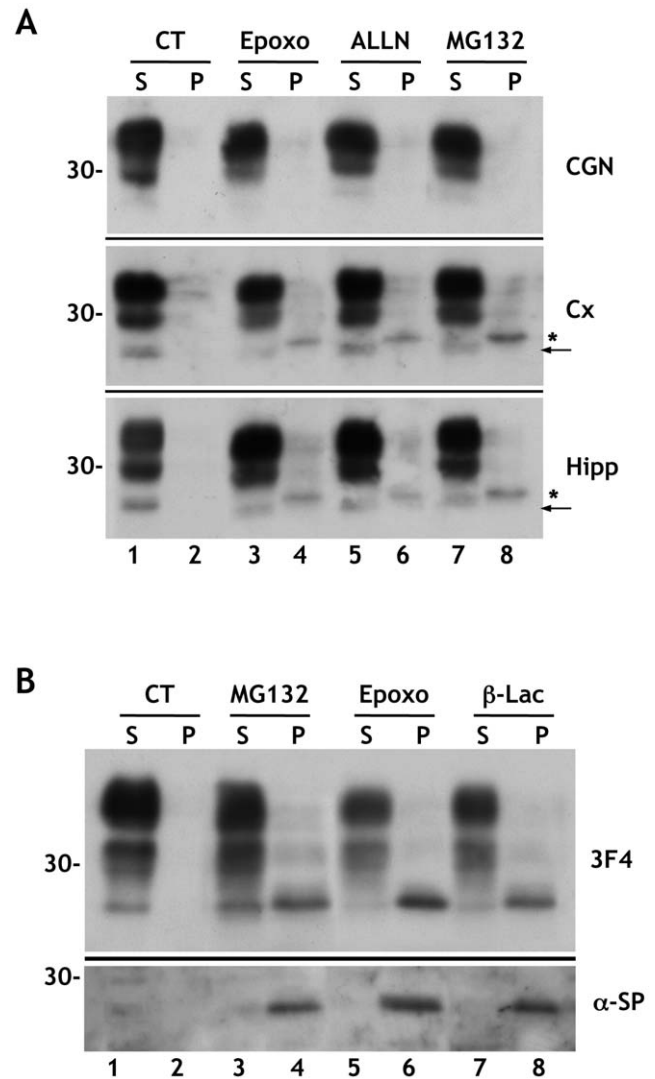


**Figure 1. Proteasome inhibitors induce accumulation of insoluble, untranslocated PrP in primary neurons.** (A) Cerebellar granule neurons (CGN), cortical (Cx) and hippocampal (Hipp) neurons from C57BL/6J mice were treated for 24h with 5  $\mu$ M epoxomicin (Epoxo), 100  $\mu$ M ALLN, 5  $\mu$ M MG132, or the vehicle alone (CT). Cell lysates were centrifuged at 186,000  $\times$  g for 40 min, and PrP in the supernatants (S) and pellets (P) was visualized by immunoblotting with antibody P45-66. The asterisks and arrows indicate bands corresponding to untranslocated PrP and mature, unglycosylated PrP, respectively. (B) Cortical neurons from Tg(WT-E1) mice were exposed to 5  $\mu$ M MG132, epoxomicin (Epoxo), lactacystin  $\beta$ -lactone ( $\beta$ -Lac) or the vehicle alone (CT). After 24 hours, cells were lysed and centrifuged at 186,000  $\times$  g for 40 min. PrP was visualized by immunoblotting with antibody 3F4 (upper panel), and with an antibody against the N-terminal signal peptide ( $\alpha$ -SP) (lower panel). Molecular mass markers are in kilodaltons. doi:10.1371/journal.pone.0013725.g001

transcripts [31,32]. Splicing was readily detected in cells treated with tunicamycin, which inhibits protein glycosylation and induces ER stress by perturbing the folding efficiency in the ER (Fig. 2A, lane 5, and 2B, lane 8). No XBP1 splicing was observed in proteasome inhibitor-treated cells (Fig. 2). There was also no increase in the ER stress-regulated protein Grp78/Bip in cells producing untranslocated PrP (data not shown). Thus, accumulation of SP-PrP was due not to an indirect effect of ER stress on PrP translocation, but to impaired degradation of a cytosolic pool of native PrP molecules.

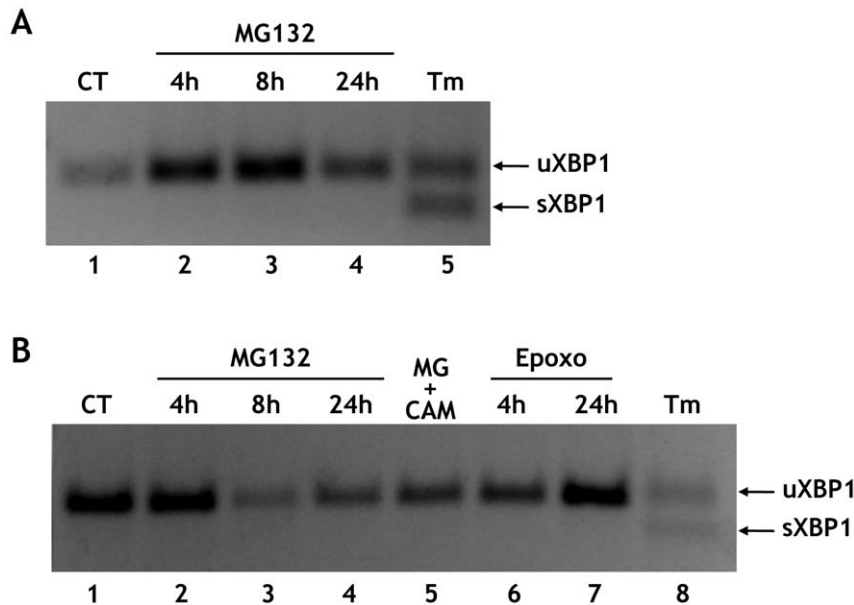


**Figure 2. Proteasome inhibitors do not induce ER stress in primary neurons.** Cortical (A) or cerebellar granule neurons (B) were treated with 5  $\mu$ M MG132 or epoxomicin (Epoxo) for the times indicated, with 5  $\mu$ M MG132 and 10  $\mu$ M CAM741 for 18 h, or 5  $\mu$ g/ml tunicamycin (Tm) for 8 h. After treatment, total RNA was extracted and analyzed by reverse transcription-PCR. XBP1 splicing was determined by the appearance of rapidly migrating spliced XBP1 in tunicamycin-treated cells. The arrows point to unspliced (uXBP1) and spliced (sXBP1) transcripts.  
doi:10.1371/journal.pone.0013725.g002

To determine the cellular localization of SP-PrP, we transfected hippocampal neurons with a plasmid encoding a PrP-enhanced green fluorescent protein (PrP-EGFP) fusion molecule [33], and induced robust synthesis of untranslocated PrP-EGFP by treating the cells with an inhibitor of PrP translocation (see below). We imaged PrP-EGFP in fixed, DAPI-stained cells by confocal microscopy to visualize its localization in relation to the nucleus. Consistent with previous immunolocalization of a non-fluorescent version of PrP in cultured neurons [15], PrP-EGFP distributed on the cell soma and along the neurites of untreated cells (Fig. 3A). There was also a fraction in intracellular compartments that co-localized with the ER and Golgi (not shown), as expected for proteins in transit towards the cell surface. In treated neurons, PrP-EGFP showed a fine punctate cytoplasmic fluorescence (Fig. 3B–D), the majority of which did not co-localize with ER or Golgi markers (Fig. 3C and D, respectively).

### Neurons Synthesizing SP-PrP Have Enhanced Resistance to Proteasome Inhibitor- and Staurosporine-induced Cell Death

To test the effect of SP-PrP on the viability of cultured neurons we used a previously described experimental paradigm [11,15]. Neurons cultured from PrP knockout ( $Pmp^{0/0}$ ) and wild-type ( $Pmp^{+/+}$ ) mice were exposed to proteasome inhibitors and their viability was evaluated after 24 h. There was no difference in viability between  $Pmp^{0/0}$  and  $Pmp^{+/+}$  CGN; in contrast, cortical and hippocampal neurons from  $Pmp^{+/+}$  mice were significantly more resistant to the inhibitors than their  $Pmp^{0/0}$  counterparts (Fig. 4A–C). Supraphysiological PrP expression further increased cortical cell resistance to the inhibitors, indicating a dose-dependent effect of PrP expression on neuronal survival (Fig. 4D). The fact that the cells that survived best were those synthesizing SP-PrP suggested that this isoform could have cytoprotective activity.

To test this, we investigated whether SP-PrP protected neurons from the toxic effect of staurosporine, a prototypic inducer of

apoptosis [34,35]. Cortical and cerebellar neurons were treated with or without MG132 for 8 hours (long enough to induce accumulation of SP-PrP in cortical cells), then incubated for 16 hours with or without staurosporine, before evaluating cell viability by MTT assay. Statistical analysis showed a significant protective effect of MG132 against staurosporine-induced cell death in cortical neurons (Fig. 5A), but no effect on CGN viability (Fig. 5B). Thus SP-PrP had an anti-apoptotic effect in cortical cells, consistent with the protective effect of cytosolic PrP against Bax-induced cell death [28,29].

### Inhibition of Protein Translocation Induces Accumulation of SP-PrP in CGN

Transgenic mice engineered to express PrP in the cytosol show massive degeneration of CGN, suggesting that cytosolic PrP may be selectively toxic to these cells [11]. To test this we sought ways to induce cytosolic PrP localization in cultured CGN. CAM741, a cyclopeptide that inhibits co-translational translocation by interfering with the correct insertion of the signal peptide into the translocon [36,37], increased the amount of SP-PrP in hippocampal and cortical neurons (Fig. 6A, compare lanes 4 and 6, and data not shown). CAM741 induced an unglycosylated PrP species in CGN (Fig. 6B, lanes 7 and 8), which was confirmed identical to SP-PrP by reactivity with the  $\alpha$ -SP antibody and an antibody directed against the C-terminal GPI-anchoring signal ( $\alpha$ -GP) [17] (Fig. 6B, right). When we analyzed how SP-PrP accumulation affected CGN viability, we found no significant difference between cells treated with MG132 alone or in combination with CAM741 (Fig. 6C), even though the latter accumulated SP-PrP (Fig. 6B, lanes 7 and 8).

Next, we tested the effect of SP-PrP in CGN deprived of serum and potassium, a condition that induces apoptotic cell death [38]. After 24 h of deprivation, CGN viability was reduced by  $\sim$ 30% (Fig. 7B). CAM741 alone, or combined with MG132 to induce accumulation of SP-PrP (Fig. 7A, lanes 7 and 8), caused a small but significant decrease of cell survival (Fig. 7B, gray bars).

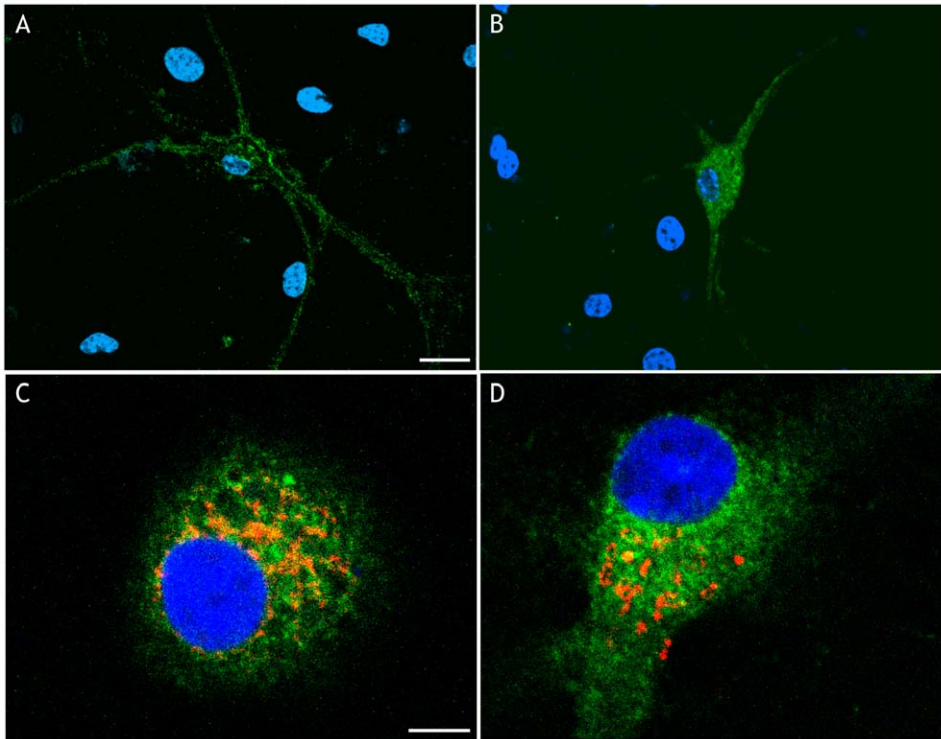


**Figure 3. Untranslocated PrP shows cytosolic localization.** Hippocampal neurons from C57BL/6J mice were transfected with a plasmid encoding PrP-EGFP (green). Twelve days after transfection cells were exposed to the vehicle (A) or treated with 10  $\mu$ M CAM741 for 24 h plus 5  $\mu$ M MG132 during the last 6 h (B–D). Cells were then fixed and reacted with DAPI (blue) to stain the nuclei. Cells in C and D were also immunostained with an anti-PDI or anti-golgin antibody (red) to visualize the ER and Golgi, respectively. Scale bar = 10  $\mu$ m in A (also applicable to B), and 5  $\mu$ m in C (also applicable to D).

doi:10.1371/journal.pone.0013725.g003

However, the same happened in CGN from *Pmp<sup>0/0</sup>* mice (Fig. 7B, white bars), indicating that the loss of cell viability was due to a toxic effect of the treatment, independent of SP-PrP.

Finally, we used an experimental paradigm similar to that shown in Fig. 5 to test whether CAM741-induced SP-PrP protected CGN from staurosporine toxicity. SP-PrP had no effect on cell viability (not shown). Thus, in CGN, SP-PrP was not toxic, and did not protect from apoptosis.

## Discussion

The cellular pathways by which cytosolic PrP is generated and the biological activity of this species have been debated. Previous investigations have used transfected cells or transgenic mice engineered to express artificial PrP molecules in the cytosol, making extrapolation to physiological conditions difficult. In the present study we investigated the biogenesis and biological activity of cytosolic PrP produced endogenously in primary neurons from different mouse brain regions. The efficiency of PrP compartmentalization in the secretory pathway varied significantly for different neurons, with cortical and hippocampal cells synthesizing an untranslocated form of cytosolic PrP, which was not present in cerebellar granules. Synthesis of untranslocated PrP caused no toxicity to neurons –in fact, it increased resistance to apoptosis. These data indicate that inefficient co-translational translocation during biogenesis is the primary source of cytosolic PrP in neurons, and raise the possibility that cytosolic targeting of nascent PrP molecules might be physiologically regulated for cellular benefit.

Proteasome inhibitors induced accumulation of an unglycosylated form of PrP in primary neurons. This form had a higher

molecular mass than mature, unglycosylated PrP and carried the N- and C-terminal signals that are cleaved in the ER lumen. Thus, cytosolic PrP represents untranslocated molecules that have never entered the ER rather than retrogradely translocated PrP, which would lack both signal peptides. In cultured neurons untranslocated PrP showed a fine punctate cytosolic localization reminiscent of that in certain brain neurons [20,21,22].

ER stress favors accumulation of untranslocated PrP by activating a “preemptive” quality control mechanism that inhibits protein translocation [17,18]. Therefore it was important to verify whether proteasome inhibitors activated ER stress pathways in neuronal cells [39]. There was no evidence of splicing of the mRNA encoding XBP-1 or increases in the levels of the ER stress-regulated protein Grp78/BiP. This indicated that SP-PrP accumulation in response to proteasome inhibition was due not to an indirect effect of ER stress, but to a pool of short-lived PrP molecules in the cytosol.

Unlike cortical and hippocampal cells, we detected no SP-PrP in cerebellar granules unless translocation was pharmacologically inhibited. This is in line with analyses of the mouse brain, where cytosolic PrP was detected in neurons of the neocortex and hippocampus, but not the cerebellum [20,21], and suggests that cell-specific factors influence PrP translocation. Consistent with this conclusion, the efficiency of PrP compartmentalization in the secretory pathway varied markedly in different cell lines [40].

The molecular steps leading to signal-mediated protein segregation into the mammalian ER include recognition of the nascent polypeptide chain by the signal recognition particle (SRP), followed by SRP-dependent targeting to the ER membrane and transfer to the Sec61 translocon. The nascent polypeptide is then inserted into the protein-conducting channel of the translocon, allowing protein

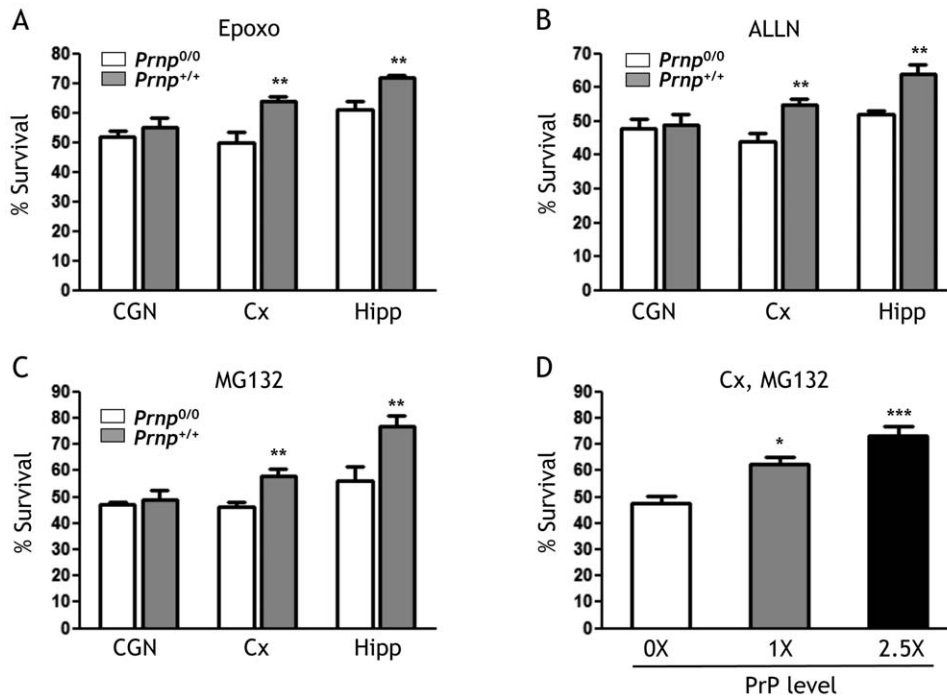


**Figure 4. Neurons synthesizing SP-PrP are more resistant to proteasome inhibitors.** Cerebellar granule neurons (CGN), cortical (Cx) and hippocampal (Hipp) neurons prepared from C57BL/6J (*Prnp*<sup>+/+</sup>) and PrP knockout (*Prnp*<sup>0/0</sup>) mice were exposed to 1  $\mu$ M epoxomicin (A), 100  $\mu$ M ALLN (B) or 5  $\mu$ M MG132 (C). Cell survival was quantified after 24 h by MTT assay and expressed as a percentage of the values for cells treated with the vehicle. Data are the mean  $\pm$  SEM of 12–24 replicates from 2–4 independent experiments; \*\* $p$ <0.01 by Tukey-Kramer test. (D) Cortical neurons were prepared from *Prnp*<sup>0/0</sup> (PrP level: 0X), *Prnp*<sup>+/+</sup> (PrP level: 1X), and Tg(WT-E1)<sup>+/-</sup>/*Prnp*<sup>+/0</sup> (PrP level:  $\sim$ 2.5X) littermates obtained by crossing Tg(WT-E1)<sup>+/-</sup>/*Prnp*<sup>+/0</sup> and *Prnp*<sup>+/0</sup> mice. Cell viability was analyzed after 24-h treatment with 5  $\mu$ M MG132 and expressed as a percentage of the values for cells treated with the vehicle. Data are the mean  $\pm$  SEM of 8–23 replicates from 2 independent experiments; \* $p$ <0.05, \*\*\* $p$ <0.001 by Dunnett's test.

doi:10.1371/journal.pone.0013725.g004

translocation concurrently with its synthesis [41]. The fact that the amount of SP-PrP increased in response to CAM741, which interferes with the correct insertion of the signal peptide into the translocon [36,37], suggests that a post-targeting interaction between the signal and the Sec61 channel is primarily involved in PrP translocation, a conclusion also emerging from other studies [18,42].

Several “accessory” components influence post-targeting PrP translocation, such as the translocon-associated protein complex TRAP [43], and chaperones and disulfide isomerases that associate with the cytoplasmic side of Sec61 [44]. It remains to be established whether regulated expression of these proteins governs SP-PrP synthesis in neuronal cells.

Consistent with evidence of an anti-apoptotic function of cytosolic PrP [28], SP-PrP protected neurons against the toxicity of proteasome inhibitors and staurosporine, which activate the intrinsic apoptotic pathway [35,45]. This effect was seen in cortical and hippocampal cells, but not in cerebellar granules where CAM741 induced SP-PrP. This suggests there are specific factors that influence the activity of SP-PrP, for example PrP-interacting proteins that may be selectively expressed or functionally more critical in some cell types than others. A number of proteins have been identified that could interact with PrP in the cytosol and mediate neuroprotection, including the anti-apoptotic protein Bcl-2 [46] and the neurotrophin receptor-interacting MAGE homologue, NRAGE [47]. However, preliminary attempts to identify a physical interaction between SP-PrP and these candidate proteins have not been rewarding (unpublished data). The fact that untranslocated PrP has a short half-life [14] suggests it may engage only in transient interactions.

The neuroprotective activity of untranslocated PrP produced endogenously in cultured neurons contrasts with the neurotoxicity of forced cytosolic PrP expression by transgenesis. A PrP construct lacking N- and C-terminal signal peptides, designed to mimic cytosolic PrP from retrotranslocation, caused massive degeneration of CGN in transgenic mice [11]. Although this observation is provocative, the lack of evidence of cytosolic PrP generation by retrotranslocation in neuronal cells [14,15, and this study] raises questions about its pathologic importance.

Rane and colleagues generated Tg mice expressing a variant of hamster PrP carrying the interferon- $\gamma$  signal peptide (Ifn-PrP), which was constitutively translocated at low levels [19]. Transgenic mice expressing small amounts of Ifn-PrP (1/6th of the endogenous PrP mRNA level) were smaller than non-Tg littermates and developed mild ataxia with modest spongiform changes at 18–24 months of age. Tg lines with higher Ifn-PrP expression could not be established because of embryonic and neonatal lethality [19]. This indicates that constitutive expression of untranslocated PrP during development is highly detrimental, perhaps underscoring the importance of regulated PrP translocation early in the mouse's life.

The signal sequence of PrP has evolved to maintain a slight but measurable inefficiency in interaction with the translocon [42,48]. This allows generation of multiple topological forms of the protein, including untranslocated PrP and <sup>C<sub>int</sub></sup>PrP, a transmembrane variant with neurotoxic properties [49,50,51]. It is therefore tempting to speculate that PrP might have acquired the ability to adopt cytosolic or transmembrane topologies with opposite effects on neuronal survival for a functional purpose, perhaps to fine-tune

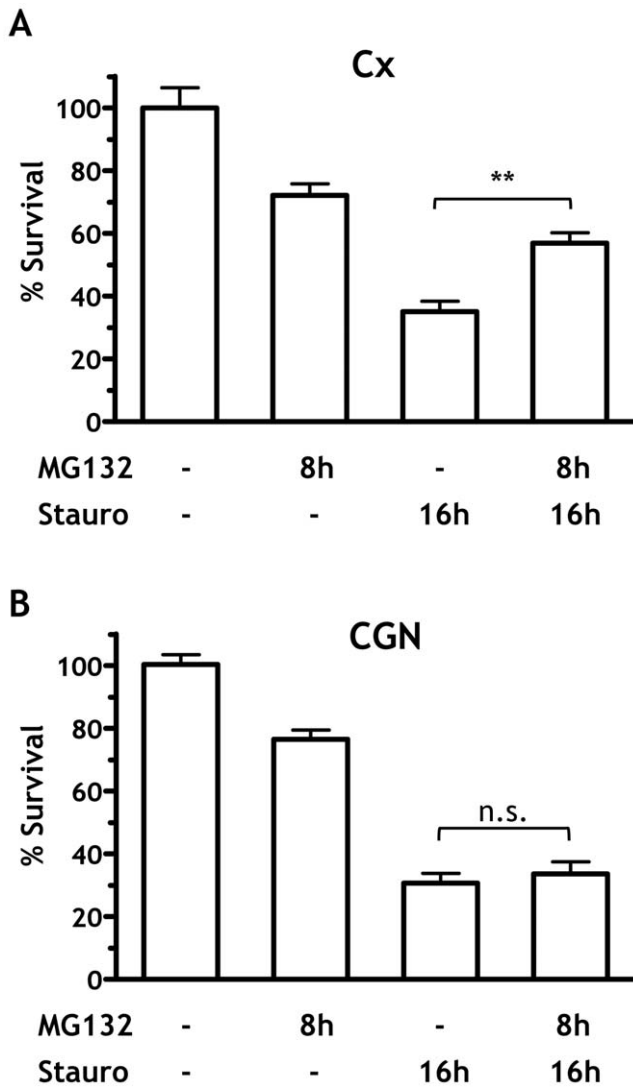


**Figure 5. MG132 protects cortical but not cerebellar granule neurons from staurosporine-induced cell death.** Cortical (A, Cx) and cerebellar granule neurons (B, CGN) from C57BL/6J mice were exposed to 5  $\mu$ M MG132 for 8 h to induce accumulation of SP-PrP in cortical neurons, and treated with 100 nM staurosporine or not for 16 h. Cell survival was quantified at the end of the treatment (24 h) by MTT assay and expressed as a percentage of the values for cells treated with the vehicle. Data are the mean  $\pm$  SEM of 20–25 replicates from four independent experiments; \*\* $p$ <0.01 by Bonferroni test. doi:10.1371/journal.pone.0013725.g005

signaling cascades that control cell fate in the developing brain [2,52]. In certain species cytosolic PrP can be generated by alternative initiation of translation, which produces PrP molecules with short signal peptides unable to negotiate entry into the ER [53,54]. Thus different molecular strategies might have evolved to produce untranslocated PrP.

A number of secretory and membrane proteins appear to have inefficient signal sequences for beneficial functions. Thus, during ER stress, proteins such as PrP are prevented from entering the secretory pathway to alleviate the burden of the folding and secretory transport machineries of the cell [17,18]. We have provided evidence that a pool of untranslocated cytosolic PrP is synthesized in certain neurons in the absence of ER stress, indicating the existence of cell type-specific pathways that control PrP translocation in physiological conditions. We also report a

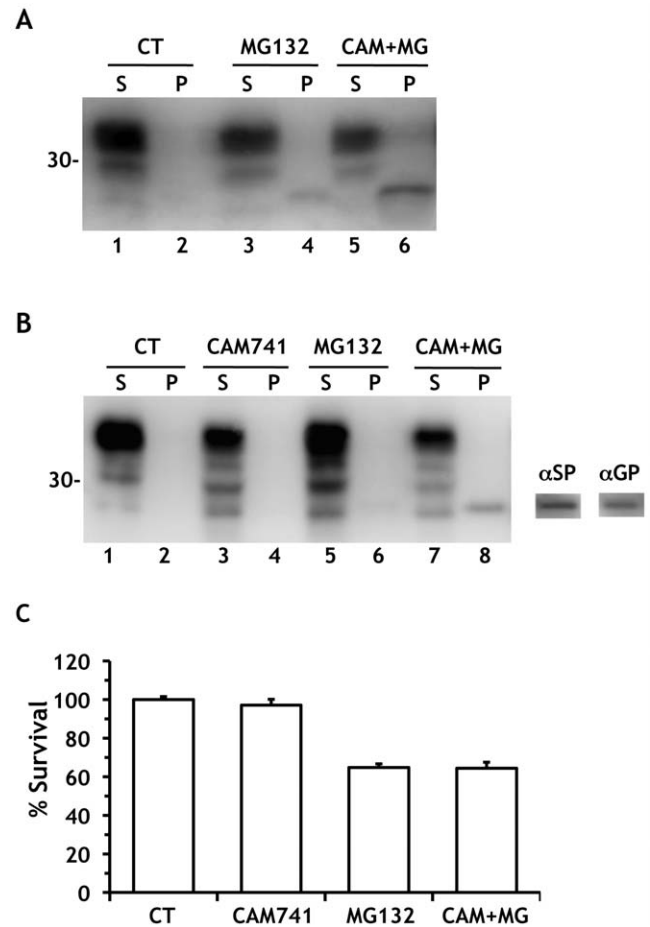


**Figure 6. SP-PrP has no effect on viability of cerebellar granule neurons.** (A) Hippocampal neurons from C57BL/6J mice were treated with 5  $\mu$ M MG132 alone or with 10  $\mu$ M CAM741 for 18 h, and PrP was analyzed by Western blot as described in the legend to Fig. 1. Note the higher level of SP-PrP in the presence of CAM741 (compare lanes 4 and 6). (B) Cerebellar granule neurons from C57BL/6J mice were treated with 10  $\mu$ M CAM741, 10  $\mu$ M MG132 or with the two drugs simultaneously for 24 h, before Western blot analysis with antibody 12B2. The PrP band in lane 8 also reacted with the  $\alpha$ -SP and  $\alpha$ -GP antibodies (on the right). (C) Cell survival was quantified by MTT assay and expressed as a percentage of the values for cells treated with the vehicle. Data are the mean  $\pm$  SEM of 18–20 replicates from two independent experiments. The Bonferroni test did not find any difference between MG132 and CAM+MG groups. doi:10.1371/journal.pone.0013725.g006

beneficial effect of untranslocated PrP on neuronal survival, suggesting a new teleological argument for the evolutionary conserved inefficiency of the PrP signal sequence. The challenge for future studies will be to elucidate the cellular mechanisms regulating the biogenesis of untranslocated PrP, and the downstream molecular pathways that mediate its biological effect.

## Materials and Methods

### Mice

Production of Tg(WT-E1) mice overexpressing mouse wild-type PrP (moPrP) tagged with an epitope for the monoclonal antibody 3F4 has been reported elsewhere [55]. *Pmp*<sup>0/0</sup> mice [56] with a pure C57BL/6J background were obtained from the European Mouse Mutant Archive (Monterotondo, Rome, Italy). C57BL/6J mice were purchased from Charles River Laboratories.

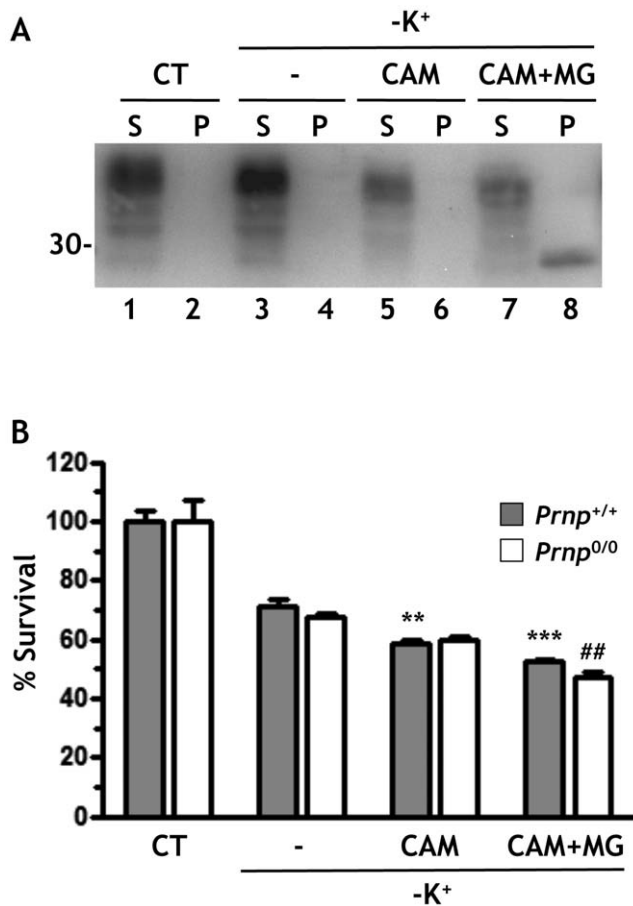


**Figure 7. SP-PrP does not affect the cerebellar granule neurons' response to serum and potassium deprivation.** (A) Cerebellar granule neurons from C57BL/6J mice were shifted to serum-free medium containing 5 mM KCl, and left untreated (-) or treated with 10  $\mu$ M CAM741 alone or in combination with 10  $\mu$ M MG132 to induce accumulation of SP-PrP. After 24 h cells were analyzed by Western blot with antibody 12B2 to verify the induction of SP-PrP. (B) Cell survival was quantified by MTT assay and expressed as a percentage of the values for untreated cells. Data are the mean  $\pm$  SEM of 12 replicates; \*\* $p$ <0.01, \*\*\* $p$ <0.001 vs -K<sup>+</sup> in Prnp<sup>+/+</sup>; ## $p$ <0.01 vs -K<sup>+</sup> in Prnp<sup>0/0</sup> by Bonferroni test. doi:10.1371/journal.pone.0013725.g007

### Ethics Statement

All procedures involving animals were conducted according to European Union (EEC Council Directive 86/609, OJ L 358,1; December 12, 1987) and Italian (D.L. n.116, G.U. suppl. 40, February 18, 1992) laws and policies, and were in accordance with the United States Department of Agriculture Animal Welfare Act and the National Institutes of Health Policy on Humane Care and Use of Laboratory Animals. They were reviewed and approved by the Mario Negri Institute Animal Care and Use Committee that includes *ad hoc* members for ethical issues (ID 9/1/01). Animal facilities meet international standards and are regularly checked by a certified veterinarian who is responsible for health monitoring, animal welfare supervision, experimental protocols and review of procedures.

### Cell Culture

Primary neuronal cultures were prepared as previously described [15,57]. Briefly, cerebella were dissected, sliced into  $\sim$ 1-mm pieces and incubated in Hank's balanced salt solution (HBSS, Gibco) containing 0.3 mg/ml trypsin (Sigma) at 37°C for

15 min. Trypsin inhibitor (Sigma) was added to a final concentration of 0.5 mg/ml and the tissue was mechanically dissociated by passing through a flame-polished Pasteur pipette. Cells were plated at 350–400,000 cells/cm<sup>2</sup> on poly-L-lysine (0.1 mg/ml)-coated plates. Cells were maintained in Basal Medium Eagle (Gibco) supplemented with 10% dialyzed fetal bovine serum (FBS, Sigma), penicillin/streptomycin and KCl 25 mM, at 37°C in an atmosphere of 5% CO<sub>2</sub>, 95% air.

Cortical and hippocampal neurons were prepared from two-day-old animals as described [57]. Brain tissue was sliced into  $\sim$ 1-mm pieces and incubated in HBSS (Gibco) containing 20 U/ml papain (Sigma) at 34°C for 30 min. Trypsin inhibitor (Sigma) was added to a final concentration of 0.5 mg/ml and the tissue was mechanically dissociated by passing through a flame-polished Pasteur pipette. Cells were plated at 150–250,000 cells/cm<sup>2</sup> on poly-D-lysine-coated (25  $\mu$ g/ml) plates and maintained in Neurobasal Basal Medium (Gibco) supplemented with B27 (Gibco), penicillin/streptomycin and glutamine 2 mM. To reduce the number of non-neuronal cells, aphidicolin (3.3  $\mu$ g/ml, Sigma) was added to the medium 48 h after plating. Non-neuronal contamination was less than 3%.

Cell viability was assessed by measuring the cellular reduction of 3-(4,5-dimethylthiazol-2-yl)-2,5-diphenyl tetrazolium bromide (MTT) to formazan [57]. Cells were incubated for 3 h at 37°C with 0.4 mg/ml MTT, dissolved in 0.04N HCl in 2-propanol, and analyzed spectrophotometrically at 540 nm with an automatic microplate reader (Labsystems Multiskan MS).

### Cell Transfection

Hippocampal neurons were transfected with a plasmid encoding a moPrP molecule containing a monomerized version of enhanced green fluorescent protein (EGFP) inserted after codon 34 [33], using the Nucleofector device and the Mouse Neuron Nucleofector Kit (Lonza). Cells were then pelleted, resuspended in RPMI 1640 (Gibco) containing 10% FBS (Sigma) and 2 mM glutamine, and plated at 300,000 cells/cm<sup>2</sup> on poly-D-lysine (25  $\mu$ g/ml)-coated plates. After 2 h the medium was replaced with Neurobasal Basal Medium (Gibco) supplemented with B27 (Gibco), penicillin/streptomycin and glutamine 2 mM, and cells were maintained at 37°C in an atmosphere of 5% CO<sub>2</sub>, 95% air. They were analyzed after 12–14 days in culture.

### Antibodies

Monoclonal antibody 3F4 was diluted 1:5,000 [58]. Rabbit polyclonal antibody P45-66, raised against a synthetic peptide encompassing residues 45–66 of moPrP, was used at 1:2,500 [59]. An affinity-purified rabbit polyclonal antibody ( $\alpha$ -SP) that selectively recognizes forms of moPrP containing an uncleaved signal peptide was used at 1:150 [30]. A rabbit polyclonal antibody ( $\alpha$ -GP) raised against the C-terminal sequence of moPrP, which is removed before the addition of the GPI anchor was used at 1:1,000 [17]. Monoclonal antibody 12B2 against moPrP sequence 88–92 was used at 1:5,000 [60]. Polyclonal rabbit antibodies against protein disulfide isomerase (PDI, Sigma) and giantin (Covance) were used at 1:500.

### Biochemical Analysis

To assay detergent insolubility, cells were lysed in 10 mM Tris pH 7.5, 100 mM NaCl, 0.5% sodium deoxycholate and 0.5% Nonidet P-40 containing protease inhibitors (pepstatin and leupeptin, 1  $\mu$ g/ml; phenylmethylsulfonyl fluoride, 0.5 mM; and ethylenediaminetetraacetic acid, 2 mM). Lysates corresponding to 300  $\mu$ g of protein were centrifuged at 186,000  $\times g$  for 40 min in a Beckman Optima Max-E ultracentrifuge. Proteins in the pellet

and supernatant were separated by sodium dodecyl sulphate-polyacrylamide gel electrophoresis and electro-transferred onto polyvinylidene fluoride membranes (Immobilon P, Millipore). Membranes were incubated first with 5% non-fat dry milk in 100 mM Tris pH 7.5, 150 mM NaCl and 0.1% Tween 20 (TTBS), then with anti-PrP antibodies overnight at 4°C or 1 h at room temperature, rinsed three times with TTBS and incubated 1 h at room temperature with horseradish peroxidase-conjugated secondary antibody (diluted 1:5,000; Santa Cruz). Signals were revealed using enhanced chemiluminescence (Amersham Biosciences), and visualized by a Biorad XRS image scanner. Quantitative densitometry of protein bands was done using Quantity One software (Biorad).

### XBP1 Splicing

Total RNA was extracted using a commercial kit (SV Total RNA Isolation System; Promega, Madison, WI), according to the manufacturer's instructions. RNA samples were reverse-transcribed with MuLV Reverse Transcriptase (Applied Biosystems) by priming with oligo(dT). XBP1 mRNA was amplified with primers flanking the 26b intron (5'-GGAGTGGAGTAAG-GCTGGTG and 5'-CCAGAAATGCCAAAAGGATA) and PCR products resolved on 2.5% agarose gels [17].

### References

- Harris DA, Lele P, Snider WD (1993) Localization of the mRNA for a chicken prion protein in situ hybridization. *Proc Natl Acad Sci U S A* 90: 4309–4313.
- Manson J, West JD, Thomson V, McBride P, Kaufman MH, et al. (1992) The prion protein gene: a role in mouse embryogenesis? *Development* 115: 117–122.
- Moser M, Colello RJ, Pott U, Oesch B (1995) Developmental expression of the prion protein gene in glial cells. *Neuron* 14: 509–517.
- Prusiner SB (1998) Prions. *Proc Natl Acad Sci U S A* 95: 13363–13383.
- Chakrabarti O, Ashok A, Hegde RS (2009) Prion protein biosynthesis and its emerging role in neurodegeneration. *Trends Biochem Sci* 34: 287–295.
- Orsi A, Sitia R (2007) Interplays between covalent modifications in the endoplasmic reticulum increase conformational diversity in nascent prion protein. *Prion* 1: 236–242.
- Campana V, Samataro D, Zurzolo C (2005) The highways and byways of prion protein trafficking. *Trends Cell Biol* 15: 102–111.
- Yedidia Y, Horonchik L, Tzaban S, Yanai A, Taraboulos A (2001) Proteasomes and ubiquitin are involved in the turnover of the wild-type prion protein. *Embo J* 20: 5383–5391.
- Ma J, Lindquist S (2001) Wild-type PrP and a mutant associated with prion disease are subject to retrograde transport and proteasome degradation. *Proc Natl Acad Sci U S A* 98: 14955–14960.
- Vembar SS, Brodsky JL (2008) One step at a time: endoplasmic reticulum-associated degradation. *Nat Rev Mol Cell Biol* 9: 944–957.
- Ma J, Wollmann R, Lindquist S (2002) Neurotoxicity and neurodegeneration when PrP accumulates in the cytosol. *Science* 298: 1781–1785.
- Wang X, Bowers SL, Wang F, Pu XA, Nelson RJ, et al. (2009) Cytoplasmic prion protein induces forebrain neurotoxicity. *Biochim Biophys Acta* 1792: 555–563.
- Faas H, Jackson WS, Borkowski AW, Wang X, Ma J, et al. (2009) Context-dependent perturbation of neural systems in transgenic mice expressing a cytosolic prion protein. *Neuroimage* 49: 2607–2617.
- Drisaldi B, Stewart RS, Adles C, Stewart LR, Quaglio E, et al. (2003) Mutant PrP is delayed in its exit from the endoplasmic reticulum, but neither wild-type nor mutant PrP undergoes retrotranslocation prior to proteasomal degradation. *J Biol Chem* 278: 21732–21743.
- Fioriti L, Dossena S, Stewart LR, Stewart RS, Harris DA, et al. (2005) Cytosolic prion protein (PrP) is not toxic in N2a cells and primary neurons expressing pathogenic PrP mutations. *J Biol Chem* 280: 11320–11328.
- Rane NS, Yonkovich JL, Hegde RS (2004) Protection from cytosolic prion protein toxicity by modulation of protein translocation. *Embo J* 23: 4550–4559.
- Orsi A, Fioriti L, Chiesa R, Sitia R (2006) Conditions of endoplasmic reticulum stress favor the accumulation of cytosolic prion protein. *J Biol Chem* 281: 30431–30438.
- Kang SW, Rane NS, Kim SJ, Garrison JL, Taunton J, et al. (2006) Substrate-specific translocational attenuation during ER stress defines a pre-emptive quality control pathway. *Cell* 127: 999–1013.
- Rane NS, Kang SW, Chakrabarti O, Feigenbaum L, Hegde RS (2008) Reduced translocation of nascent prion protein during ER stress contributes to neurodegeneration. *Dev Cell* 15: 359–370.

### Immunofluorescence Staining

Cells grown on 8-well 15- $\mu$ m slides (Ibidi, Martinsried, Germany) were washed with phosphate buffered saline (PBS) and fixed for 30 min at room temperature with 4% paraformaldehyde in PBS. They were then washed with PBS, incubated with blocking solution containing 0.1% saponin, 0.5% BSA, 50 mM NH<sub>4</sub>Cl in PBS, and with primary and Alexa (Molecular Probes)-conjugated secondary antibodies diluted in the same solution. Cells were stained with 1  $\mu$ g/ml DAPI (Sigma Aldrich) for 5 min and analyzed with an Olympus FV500 laser confocal scanning system.

### Acknowledgments

We thank Richard Kascsak (Institute for Basic Research in Developmental Disabilities, Staten Island, NY, USA) for 3F4 antibody, David A. Harris (Boston University, Boston, MA, USA) for the P45-66,  $\alpha$ -SP and  $\alpha$ -GP antibodies, and Jan Langeveld (Central Veterinary Institute of Wageningen UR, Lelystad, The Netherlands) for the 12B2 antibody. We are grateful to Novartis Pharma AG (Basel, Switzerland) for providing CAM741.

### Author Contributions

Conceived and designed the experiments: RC. Performed the experiments: ER LF SM SA. Analyzed the data: ER LF GF. Wrote the paper: RC.

- Mironov A, Jr., Latawiec D, Wille H, Bouzamondo-Bernstein E, Legname G, et al. (2003) Cytosolic prion protein in neurons. *J Neurosci* 23: 7183–7193.
- Barmada S, Piccardo P, Yamaguchi K, Ghetti B, Harris DA (2004) GFP-tagged prion protein is correctly localized and functionally active in the brains of transgenic mice. *Neurobiol Dis* 16: 527–537.
- Bailly Y, Haeblerle AM, Blanquet-Grossard F, Chasserot-Golaz S, Grant N, et al. (2004) Prion protein (PrP<sup>C</sup>) immunocytochemistry and expression of the green fluorescent protein reporter gene under control of the bovine PrP gene promoter in the mouse brain. *J Comp Neurol* 473: 244–269.
- Grenier C, Bissonnette C, Volkov L, Roucou X (2006) Molecular morphology and toxicity of cytoplasmic prion protein aggregates in neuronal and non-neuronal cells. *J Neurochem* 97: 1456–1466.
- Rambold AS, Miesbauer M, Rapaport D, Bartke T, Baier M, et al. (2006) Association of Bcl-2 with misfolded prion protein is linked to the toxic potential of cytosolic PrP. *Mol Biol Cell*.
- Wang X, Dong CF, Shi Q, Shi S, Wang GR, et al. (2009) Cytosolic prion protein induces apoptosis in human neuronal cell SH-SY5Y via mitochondrial disruption pathway. *BMB Rep* 42: 444–449.
- Kristiansen M, Messenger MJ, Klohn PG, Brandner S, Wadsworth JD, et al. (2005) Disease-related prion protein forms aggregates in neuronal cells leading to caspase activation and apoptosis. *J Biol Chem* 280: 38851–38861.
- Crozet C, Vezilier J, Delfieu V, Nishimura T, Onodera T, et al. (2006) The truncated 23-230 form of the prion protein localizes to the nuclei of inducible cell lines independently of its nuclear localization signals and is not cytotoxic. *Mol Cell Neurosci*.
- Roucou X, Guo Q, Zhang Y, Goodyer CG, LeBlanc AC (2003) Cytosolic prion protein is not toxic and protects against Bax-mediated cell death in human primary neurons. *J Biol Chem* 278: 40877–40881.
- Lin DT, Jodoin J, Baril M, Goodyer CG, LeBlanc AC (2008) Cytosolic prion protein is the predominant anti-Bax prion protein form: exclusion of transmembrane and secreted prion protein forms in the anti-Bax function. *Biochim Biophys Acta* 1783: 2001–2012.
- Stewart RS, Harris DA (2003) Mutational analysis of topological determinants in PrP, and measurement of transmembrane and cytosolic PrP during prion infection. *J Biol Chem* 278: 45960–45968.
- Yoshida H, Matsui T, Yamamoto A, Okada T, Mori K (2001) XBP1 mRNA is induced by ATF6 and spliced by IRE1 in response to ER stress to produce a highly active transcription factor. *Cell* 107: 881–891.
- Lee K, Tirasophon W, Shen X, Michalak M, Prywes R, et al. (2002) IRE1-mediated unconventional mRNA splicing and S2P-mediated ATF6 cleavage merge to regulate XBP1 in signaling the unfolded protein response. *Genes Dev* 16: 452–466.
- Massignan T, Biasini E, Lauranzano E, Veglianesi P, Pignataro M, et al. (2010) Mutant prion protein expression is associated with an alteration of the Rab GDP dissociation inhibitor alpha (GDI)/Rab11 pathway. *Mol Cell Proteomics* 9: 611–622.
- Bertrand R, Solary E, O'Connor P, Kohn KW, Pommier Y (1994) Induction of a common pathway of apoptosis by staurosporine. *Exp Cell Res* 211: 314–321.



35. Koh JY, Wie MB, Gwag BJ, Sensi SL, Canzoniero LM, et al. (1995) Staurosporine-induced neuronal apoptosis. *Exp Neurol* 135: 153–159.
36. Besemer J, Harant H, Wang S, Oberhauser B, Marquardt K, et al. (2005) Selective inhibition of cotranslational translocation of vascular cell adhesion molecule 1. *Nature* 436: 290–293.
37. Harant H, Lettner N, Hofer L, Oberhauser B, de Vries JE, et al. (2006) The translocation inhibitor CAM741 interferes with vascular cell adhesion molecule 1 signal peptide insertion at the translocon. *J Biol Chem* 281: 30492–30502.
38. Miller TM, Johnson EM, Jr. (1996) Metabolic and genetic analyses of apoptosis in potassium/serum-deprived rat cerebellar granule cells. *J Neurosci* 16: 7487–7495.
39. Kaufman RJ (2002) Orchestrating the unfolded protein response in health and disease. *J Clin Invest* 110: 1389–1398.
40. Levine CG, Mitra D, Sharma A, Smith CL, Hegde RS (2005) The efficiency of protein compartmentalization into the secretory pathway. *Mol Biol Cell* 16: 279–291.
41. Rapoport TA (2007) Protein translocation across the eukaryotic endoplasmic reticulum and bacterial plasma membranes. *Nature* 450: 663–669.
42. Rutkowski DT, Lingappa VR, Hegde RS (2001) Substrate-specific regulation of the ribosome-translocon junction by N-terminal signal sequences. *Proc Natl Acad Sci U S A* 98: 7823–7828.
43. Fons RD, Bogert BA, Hegde RS (2003) Substrate-specific function of the translocon-associated protein complex during translocation across the ER membrane. *J Cell Biol* 160: 529–539.
44. Stockton JD, Merkert MC, Kellaris KV (2003) A complex of chaperones and disulfide isomerases occludes the cytosolic face of the translocation protein Sec61p and affects translocation of the prion protein. *Biochemistry* 42: 12821–12834.
45. Lang-Rollin I, Vekrellis K, Wang Q, Rideout HJ, Stefanis L (2004) Application of proteasomal inhibitors to mouse sympathetic neurons activates the intrinsic apoptotic pathway. *J Neurochem* 90: 1511–1520.
46. Kurschner C, Morgan JI (1995) The cellular prion protein (PrP) selectively binds to Bcl-2 in the yeast two-hybrid system. *Brain Res Mol Brain Res* 30: 165–168.
47. Bragason BT, Palsdottir A (2005) Interaction of PrP with NRAGE, a protein involved in neuronal apoptosis. *Mol Cell Neurosci* 29: 232–244.
48. Kim SJ, Hegde RS (2002) Cotranslational partitioning of nascent prion protein into multiple populations at the translocation channel. *Mol Biol Cell* 13: 3775–3786.
49. Hegde RS, Mastrianni JA, Scott MR, DeFea KA, Tremblay P, et al. (1998) A transmembrane form of the prion protein in neurodegenerative disease. *Science* 279: 827–834.
50. Hegde RS, Tremblay P, Groth D, DeArmond SJ, Prusiner SB, et al. (1999) Transmissible and genetic prion diseases share a common pathway of neurodegeneration. *Nature* 402: 822–826.
51. Stewart RS, Piccardo P, Ghetti B, Harris DA (2005) Neurodegenerative illness in transgenic mice expressing a transmembrane form of the prion protein. *J Neurosci* 25: 3469–3477.
52. Steele AD, Emsley JG, Ozdinler PH, Lindquist S, Macklis JD (2006) Prion protein (PrP<sup>C</sup>) positively regulates neural precursor proliferation during developmental and adult mammalian neurogenesis. *Proc Natl Acad Sci U S A* 103: 3416–3421.
53. Juanes ME, Elvira G, Garcia-Grande A, Calero M, Gasset M (2009) Biosynthesis of prion protein nucleocytoplasmic isoforms by alternative initiation of translation. *J Biol Chem* 284: 2787–2794.
54. Lund C, Olsen CM, Skogtvedt S, Tveit H, Prydz K, et al. (2009) Alternative translation initiation generates cytoplasmic sheep prion protein. *J Biol Chem* 284: 19668–19678.
55. Chiesa R, Piccardo P, Ghetti B, Harris DA (1998) Neurological illness in transgenic mice expressing a prion protein with an insertional mutation. *Neuron* 21: 1339–1351.
56. Bueler H, Fischer M, Lang Y, Bluethmann H, Lipp HP, et al. (1992) Normal development and behaviour of mice lacking the neuronal cell-surface PrP protein. *Nature* 356: 577–582.
57. Chiesa R, Fioriti L, Tagliavini F, Salmona M, Forloni G (2004) Cytotoxicity of PrP peptides. In: Lehmann S, Grassi J, eds. *Techniques in Prion Research*. Basel: Birkhäuser Verlag, pp 176–197.
58. Kascsak RJ, Rubenstein R, Merz PA, Tonna-DeMasi M, Fersko R, et al. (1987) Mouse polyclonal and monoclonal antibody to scrapie-associated fibril proteins. *J Virol* 61: 3688–3693.
59. Lehmann S, Harris DA (1995) A mutant prion protein displays an aberrant membrane association when expressed in cultured cells. *J Biol Chem* 270: 24589–24597.
60. Langeveld JP, Jacobs JG, Erkens JH, Bossers A, van Zijderveld FG, et al. (2006) Rapid and discriminatory diagnosis of scrapie and BSE in retro-pharyngeal lymph nodes of sheep. *BMC Vet Res* 2: 19.